



This work is distributed under the Creative Commons Attribution 4.0 License.

Received: October 29, 2021

Revision received: October 19, 2022

Accepted: October 31, 2022

Published online: December 28, 2022

## Research article

# The Upper Cretaceous (Santonian-Maastrichtian) phosphate deposits in the west of the Neiva subbasin, Upper Magdalena Valley, Colombia

El Cretácico Superior con fosfatos (Santoniano-Maastrichtiano) en el occidente de la subcuenca de Neiva, Valle Superior del Magdalena, Colombia

Claudia L. Martín Rincón<sup>1</sup>, Roberto Terraza Melo<sup>1</sup>, Nadia R. Rojas Parra<sup>1</sup>, Germán A. Martínez Aparicio<sup>1</sup>, Sandra Rojas Jiménez<sup>1</sup>, Juan S. Hernández González<sup>1</sup>

1. Dirección de Recursos Minerales, Servicio Geológico Colombiano, Bogotá, Colombia.

**Corresponding author:** Claudia Martín, [cmartin@sgc.gov.co](mailto:cmartin@sgc.gov.co)

## ABSTRACT

It has long been known that economically exploitable phosphates in Colombia are contained within the Upper Cretaceous marine sedimentary successions (Cathcart and Zambrano, 1967; Mojica, 1987; Zambrano and Mojica, 1990). In the western region of the Neiva subbasin, which lies within the Upper Magdalena Valley (UMV), these layers are restricted to the Santonian-Maastrichtian interval, which is represented by the Lidita Inferior, Lidita Superior and Yaguará formations. The phosphates are laterally discontinuous and exhibit variations in the facies over short distances. The facies analysis and the stratigraphic correlations allowed us to infer that the facies in these units represent a very shallow marine environment that occurred at the transition between the offshore zones and the upper shoreface and included the lagoonal conditions identified within the Aico Formation. It is possible that paleotopographic variability and differential subsidence affected the lateral continuity and thickness of the Santonian-Maastrichtian lithostratigraphic units. Furthermore, subsequent tectonic events may have modified the spatial distribution of the phosphate deposits. The La Plata (Chusma) fault divides the study area into two structural domains. One is located in the west, in the hanging wall, where the oldest rocks of the pre-Cretaceous basement crop out, and the other domain is located in the east, within the footwall. This footwall is where the outcrops of the Cretaceous-Quaternary sedimentary sequences characteristic of the Neiva subbasin are found. In the footwall there are important folds, such as the Media Luna syncline and the San Francisco anticline to the north, the La Guagua anticline in the central area, and the La Hocha anticline and the El Vegón syncline to the south. Some of these folds are truncated by regional reverse faults with a dextral-strike component, such as the La Plata (Chusma), San Francisco and Betania faults.

**Citation:** Martín Rincón, C. L., Terraza Melo, R., Rojas Parra, N. R., Martínez Aparicio, G. A., Rojas Jiménez, S., & Hernández González, J. S. (2022). The Upper Cretaceous (Santonian-Maastrichtian) phosphate deposits in the west of the Neiva subbasin, Upper Magdalena Valley, Colombia. *Boletín Geológico*, 49(2), 75-96. <https://doi.org/10.32685/0120-1425/bol.geol.49.2.2022.621>

**Keywords:** Phosphates, Neiva subbasin, Upper Magdalena Valley, Upper Cretaceous, facies, stratigraphy.

## RESUMEN

De tiempo atrás se conoce que los fosfatos económicamente explotables en Colombia se encuentran en sucesiones sedimentarias marinas del Cretácico Superior (Cathcart y Zambrano, 1967; Mojica, 1987; Zambrano y Mojica, 1990). En el occidente de la subcuenca de Neiva del Valle Superior del Magdalena (VSM), estos niveles están restringidos al intervalo Santoniano-Maastrichtiano, representado en las formaciones Lidita Inferior, Lidita Superior y Yaguará. Los fosfatos son lateralmente discontinuos y presentan variaciones faciales en distancias cortas. El análisis facial y las correlaciones estratigráficas permitieron inferir que las facies presentes en estas unidades representan un ambiente marino muy somero desde la zona de transición con el *offshore* hasta el *shoreface* superior, incluyendo condiciones de *laggon* para la Formación Aico. Posiblemente, la paleotopografía y la subsidencia diferencial han afectado la continuidad lateral y el espesor de las unidades litoestratigráficas del intervalo Santoniano-Maastrichtiano, y los eventos tectónicos posteriores han modificado la distribución espacial de los depósitos de fosfatos. La falla de La Plata (Chusma) divide la zona en cuestión en dos dominios estructurales: uno localizado en el occidente, en el bloque levantado, donde afloran las rocas más antiguas del basamento pre-Cretácico, y otro dominio localizado en el oriente, en el bloque hundido, donde aflora la secuencia sedimentaria cretácica-cuaternaria característica de la subcuenca de Neiva. En el bloque hundido se encuentran pliegues importantes, como el Sinclinal de Media Luna y el Anticlinal de San Francisco en el norte, el Anticlinal de La Guagua en la parte central, y el Anticlinal de La Hocha y el Sinclinal de El Vegón en el sur. Algunos de estos pliegues están truncados por fallas regionales inversas con componente de rumbo dextral, como las fallas de La Plata (Chusma), San Francisco y Betania.

**Palabras clave:** Fosfatos, subcuenca de Neiva, Valle Superior del Magdalena, Cretácico Superior, facies, estratigrafía.

## 1. INTRODUCTION

The essential chemical elements for the development of living organisms (e.g., plants and animals) are carbon, hydrogen, nitrogen, potassium, sulfur and phosphorus, being the last one used in fertilizer by the agroindustry. However, the availability of phosphorus, unlike calcium, nitrogen and potassium, is dependent solely on its extraction from rocks that contain phosphate (Soudry et al., 2006), which makes necessary its exploration. The main economically exploitable phosphate deposits worldwide were originated between the Upper Cretaceous and Eocene in the South Tethyan Phosphogenic Province (STPP), which extends from Colombia to Venezuela and from the northern and northwestern regions of Africa into the Middle East (Notholt, 1985; Follmi et al., 1992; Pufahl et al., 2003). These deposits are characteristic of an epicontinental sea on a carbonate dominated platform that extended along the margin of the STPP (Follmi et al., 1992) and constitute the largest known accumulation of sedimentary phosphorites, which is host of the 66% of the global phosphate reserves (Grimm, 1997; USGS, 2000; Pufahl et al., 2003).

In Colombia, the STPP consists of phosphate deposits that extend through the Eastern Cordillera and the southeastern

end of the Central Cordillera and involves rocks from the Catatumbo, Middle and Upper Magdalena Valley, Eastern Cordillera and Caguán-Putumayo basins. Furthermore, these deposits are located in the departments of Norte de Santander, Santander, Boyacá, Cundinamarca, Tolima, Huila and part of the departments of Putumayo and Cauca (Zambrano and Mojica, 1990; Mojica, 1987; Terraza et al., 2016, 2019).

Phosphate deposits are found in the Cretaceous sedimentary successions, which initially (i.e., the Early Cretaceous) accumulated in a *rift*-type basin with an extensional tectonic regime inherited from the Jurassic (Julivert, 1970; Bayona et al., 1994; Sarmiento, 2019). Later, at the end of the Late Cretaceous, this regime transitioned to a compressional regime and the basin was fully closed (Bayona, 2018; Zapata et al., 2019; Sarmiento, 2019).

In the western part of the Neiva subbasin in the Upper Magdalena Valley (UMV), potentially exploitable phosphate levels appear in the Lidita Inferior, Aico, Aipe, Lidita Superior and Yaguará formations (*sensu* Terraza et al., 2019) which were deposited between the Santonian and the Maastrichtian. Most of these deposits have not been characterized in detail. However, considering their economic importance for the country's agroindustry, the national government issued Conpes 3577 do-

cument in 2009, which instructed the Servicio Geológico Colombiano (SGC) to identify new potential mineral sources for the production of fertilizers, which phosphates are essential. The objective is that, in the medium term, the country will be able to manufacture and market phosphorous-based agrochemicals at more affordable prices for Colombian farmers.

For this purpose, the results of the geological exploration carried out in the western sector of the Neiva subbasin are presented, which included geological mapping at 1:25 000 scale and detailed stratigraphic descriptions of eleven stratigraphic sections. These works allowed us a better understanding of the phosphate-bearing lithostratigraphic units and to better understand the accumulation processes. Additionally, based on the comparison of those stratigraphic sections, as well as on the facies analyses and sedimentary environment analyses, we propose an outline of the possible basin paleotopography during the Santonian-Maastrichtian interval.

## 2. REGIONAL GEOLOGICAL FRAMEWORK

The UMV basin corresponds to a structural depression that is oriented along the SSW-NNE direction and is bounded on its eastern and western sides by compressive and transpressive faults (Roncancio and Martínez, 2010). In the Mesozoic, extensional tectonic events were predominant, and compressional events dominated in the Cenozoic (Mojica and Franco, 1990; Horton et al., 2010). The Cretaceous sedimentary succession was deposited in a retroarc basin that formed in the Jurassic (Bayona et al., 1994), which at the end of the Early Cretaceous transitioned from an extensional tectonic regime to a compressional regime due to the oblique subduction and accretion of oceanic crust along the continental margin (Horton et al., 2010; Bayona, 2018; Zapata et al., 2019). Subsequent tectonic events gave rise to new structures, geometric changes occurred in the preexisting structures, and some of these structures were eroded or further deformed (Roncancio and Martínez, 2010; Jiménez et al., 2012).

The Natagaima Arch, or Alto de Patá, divides the UMV in two parts: the Neiva subbasin, located in the southern part, and the Girardot subbasin, located in the northern part (Beltrán and Gallo, 1968). In the case of the Neiva subbasin, the Garzón-Suaza fault together with the western foothills of the Garzón Massif mark the eastern limit, and the La Plata (Chusma) fault together with the eastern foothills of the Central Cordillera delimit the western limit (Figure 1). The paleotopography of

the basement affected the geometric configuration of the surface structures, which is reflected in the curvilinear outline of the major fold axes, such as by the Tesalia syncline and the La Hocha anticline (Jiménez et al., 2012).

The study area is comprised of Jurassic, plutonic and volcanic igneous rocks, whose compositions vary from felsic to intermediate (i.e., Saldaña Formation, Ibagué Batholith and related igneous bodies) (Bustamante et al., 2016; Rodríguez et al., 2018; Hernández and Urueña, 2017; Villamizar et al., 2021). Unconformably on the basement, sedimentary rocks from the basal Cretaceous crop out, composed of siliciclastic sediments that range in size from sand to gravel, accumulated in a depositional environment likely consisted of alluvial fans and fluvial systems (i.e., Yaví and Alpujarra formations) (Flórez and Carrillo, 1994; Etayo, 1994).

The remaining Cretaceous sequence, deposited in transitional and shallow marine environments (Etayo, 1994), corresponds to mixed sedimentary rocks or fine texture calcareous rocks and is enriched with organic matter and planktonic or benthic foraminifera. This sequence is contained within the El Ocal, Tetuán, Bambucá, Hondita, Loma Gorda, Lidita Inferior, Aico, Lidita Superior and Yaguará formations (*sensu* Terraza et al., 2019).

The Cretaceous sequence is unconformably covered by a thick succession of Paleogene and Neogene sedimentary rocks that are predominantly fluvial in origin and are dominated by conglomerates and sandstones (from the upper part of the Seca Formation, Chicoral and Doima Formations and Honda Group), with mudstone and claystone intercalations (found in the lower part of the Seca, Potrerillo and Barzalosa formations) (Terraza et al., 2019; Villamizar et al., 2021).

## 3. METHODOLOGY

The topography used as the basis for the geological map was compiled from digital and analog sources provided by the Instituto Geográfico Agustín Codazzi (IGAC) at a 1:25 000 scale. Field trips were carried out transversally to the geological structures with four or more control points for each linear kilometer. This allowed for the different outcropping units to be described in greater detail, for the lateral variations in facies to be more accurately assessed, and for a more reliable interpretation of the geological structures. For the systematic monitoring of regional structures (faults and folds) and competent and incompetent lithostratigraphic levels or units, a 30 m resolution digital terrain

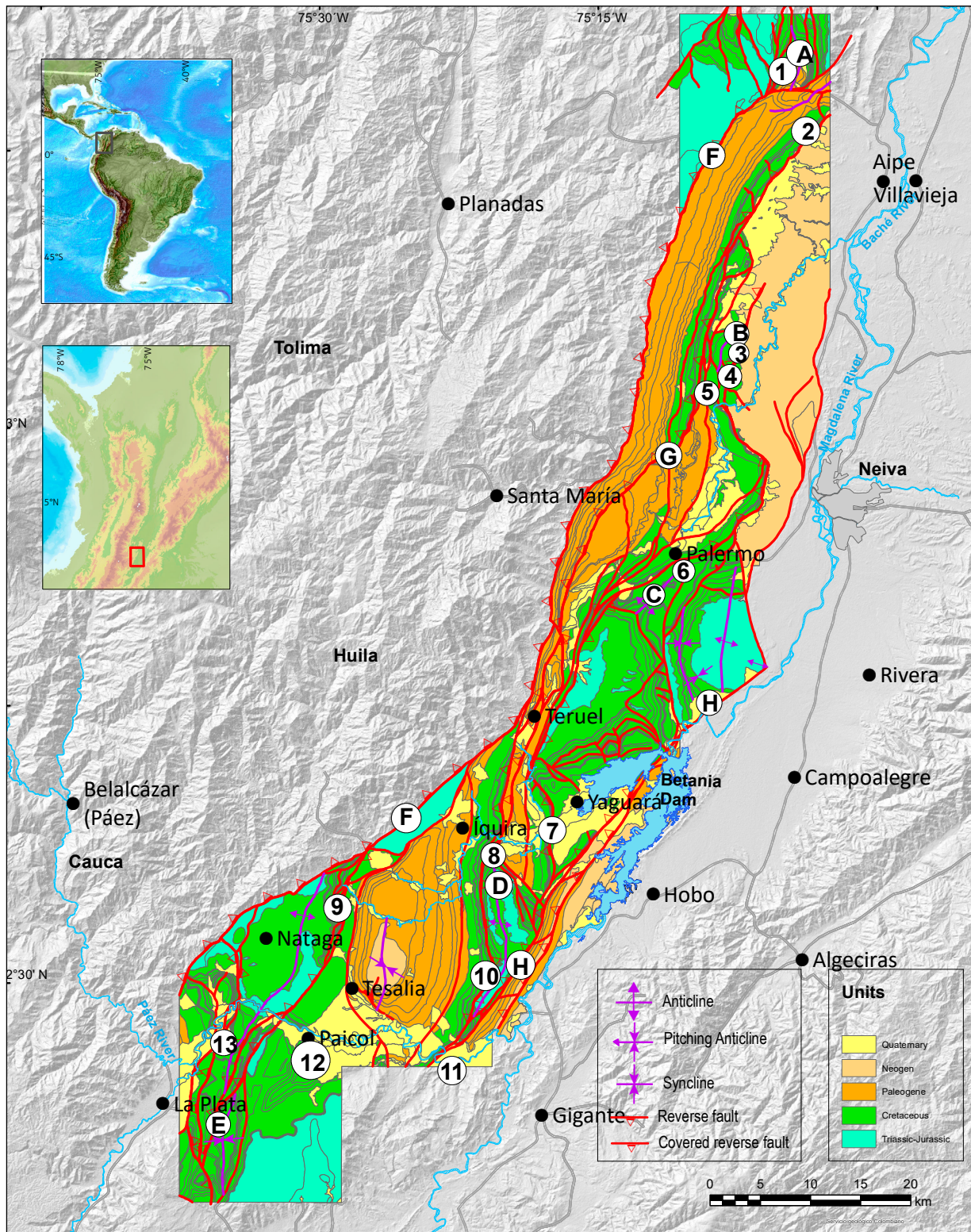


**Figure 1.** Regional geology of the study area  
 Numbers 1 to 13 show the locations of the stratigraphic sections referenced in this article: 1 = Bambucá creek, 2 = Aipe River, 3 = La Honda creek, 4 = La Tribuna, 5 = Yaya River, 6 = El Boquerón creek, 7 = Yaguará River, 8 = Íquira River, 9 = Yaguaracito River, 10 = El Caney creek, 11 = La Juanita, 12 = Divino Niño, 13 = Itaibe creek. Letters A to H: A = Media Luna Syncline, B = San Francisco Anticline, C = La Guagua Anticline, D = La Hocha Anticline, E = El Vegón Syncline, F = La Plata (Chusma) Fault, G = San Francisco Fault, H = Betania Fault

model was used, as were aerial photographs at a scale between approximately 1:22 000 and 1:43 000, which were acquired along NS-oriented flight paths, and from Google Earth imagery.

Stratigraphic columns were measured with a “Jacob’s staff”. The main rock features (color, texture, composition, layer shapes, sedimentary structures, fossils and degree of bioturbation) were recorded at 1:100 or 1:200 scales consistent with the previously discussed field formats. Field lithological descriptions were complemented by microscopic analyses of thin sections. Strike and dip data were taken with a structural type Brunton compass. Control points and sampling locations were georeferenced with a Garmin GPSmap 62s. To visualize very thin lithostratigraphic units on the geological map, such as from the Lidita Inferior and Lidita Superior formations of the Olini Group, it was necessary to exaggerate their thicknesses.

For the lithological description of the rock outcrops, by either hand samples or thin sections, the following protocols were used: 1) to determine the thickness of layers and sheets, the methods established by Ingram (1954) and Campbell (1967) and adapted by Reineck and Singh (1980) were followed; 2) to determine the type of contact between layers (sharp or gradational), geometry (tabular or wedge-shaped) and partition, the methods from Wilkins (2011) were used; 3) diagrams proposed by Krumbein and Sloss (1969) were used to identify sedimentary particle shape; 4) diagrams proposed by Compton (1985) were used to identify particles in sediments or clastic sedimentary rocks; 5) the classification of calcareous rocks was done according to Dunham (1962) and Folk (1962); 6) in order to classify terrigenous rocks according to their texture and composition, the methods described by Folk (1951, 1954, 1959, 1962, 1974) were followed; 6) the degree of bioturbation was assessed with Moore and Scruton (1957) systematics; 7) the roundness of sedimentary particles was determined by following the Powers (1953) diagram; 8) Reineck and Wunderlich (1968) diagrams were used to distinguish between lenticular and *flaser* stratification; 9) rock colors (for either wet or dry samples) were determined according to the color chart provided by The Geological Society of America (1995); 10) “mixed” rocks (i.e., rocks with a mixture of terrigenes and authigenic siliceous and calcareous components) were identified in accordance with the general classification of sedimentary rocks established by Williams et al. (1954); 11) the macroscopic description of siliceous rocks (i.e., with > 50% diagenetic or primary silica, such as cherts and porcelanites, or impure cherts) was supported by the Dunham (1962) textural classi-

fication system, e.g., chert with 10-50% of benthic foraminifera is described as fossiliferous chert of benthic foraminifera with wackestone texture; 12) phosphate rocks and phosphorites were classified according to the systematics proposed by Ptáček (2016) and Cook et al. (1986) (in Cook and Shergold, 1986), which was based on Dunham’s (1962) classification of calcareous rocks but modified for phosphorites, e.g., a phosphorite composed of peloids and fish remains with a packstone texture would represent a rock with peloids and fish fragments in a proportion >50%, whose texture resembles that of a packstone texture limestone; 13) for the identification of the phosphorus element in the samples, a qualitative chemical test was carried out with 30% HNO<sub>3</sub> and ammonium molybdate in excess (Swanson, 1981); if phosphorus is present, a yellow precipitate of ammonium phosphomolybdate is produced, the color intensity indicated that either a low, medium or high concentration of this element is present.

Lithological and facies comparison (lithocorrelation) was performed on the Upper Cretaceous stratigraphic sections of interest for the identification of phosphates. A total of eleven stratigraphic sections were developed, and the stratigraphic sections from the Itaibe creek studied by Mendivelso (1982, 1993) and the Bambucá creek described during the SGC-UNAL Agreement (2018) were included, which allowed establishing the chronostratigraphic positions of the phosphate intervals. Additionally, we relied on the advice of Professor Fernando Etayo Serna, both in the laboratory and in the field, who assisted in determining the stratigraphic positions of the different mapped lithostratigraphic units. Sections were all drawn at the same scale, and a common reference stratigraphic level was taken (e.g., the contact between the Yaguará or La Tabla formations and Seca Formation [see Figures 8, 10 and 11]) to a better analysis of the spatial distribution (lateral and vertical) of phosphate levels and visualize their relationships with other regional structures (faults and folds) and the basement. The locations of these sections are shown in Figure 1.

For the interpretation of the sedimentary environments, petrographic analyses and the main features of the layers were considered. Additionally, the grain size and composition, geometry, thickness, type of contact, sedimentary structures, fossil content, degree of bioturbation, and some paleoenvironmental indicators, such as glauconite or siderite, were also considered. The methods and techniques followed can be found in Reineck and Singh (1980), Van Wagoner et al. (1990), Kamola and Van Wagoner (1995) and Hampson and Storms (2003).

## 4. RESULTS

### 4.1. Description of the main folds and faults

The most important structures are the Media Luna syncline, the San Francisco anticline and the San Francisco fault in the north; the La Guagua anticline in the central part; and the La Hocha anticline and the El Vegón syncline to the south. Finally, the La Plata (Chusma) fault and the Betania fault are regional structures that cross the study area from south to north (see Figure 1 for their locations).

**Media Luna syncline.** This syncline is a fold isolated by faulting and surrounded by the pre-Cretaceous basement located in the hanging wall of the La Plata (Chusma) fault. It is a subvertical and open fold whose axial plane presents a dip greater than  $80^\circ$  to the west and a moderate dip to the SW. It follows an elongated “S” shape and ends to the north against the Jurassic basement of the Saldaña Formation and to the SW against the La Plata (Chusma) fault. At the core are rocks from the Seca Formation and on its flanks Cretaceous rocks are outcropping, from the Alpujarra Formation to La Tabla Formation (Figures 2a, 2b).

**San Francisco anticline.** Is a complex fold that varies from subvertical and open to sloping and asymmetric, with moderate dipping in both the NE and south; its axis is slightly sinuous and curved along a NE and SE direction. It is truncated by some thrust faults with a dextral-strike component that produce axial displacement. The Baché fault abruptly cuts the eastern flank and the southern end of the fold, and the western flank is cut by the San Francisco fault (Figure 2c). Rocks from the Loma Gorda Formation crop out in the core and rocks from the Olini Group and Yaguará Formation crop out on the flanks.

**La Guagua anticline.** This anticline consists of a smooth vertical fold, dipping weakly to the NNE and a general NNE orientation. Geographically, the anticline is confined between the Upar and Baché faults to the west and La Boa fault to the east. Jurassic plutons crop out in the center of the structure and the entire Cretaceous succession and part of the Paleogene succession overlay those plutons.

**La Hocha anticline.** This anticline consists of a vertical fold with structural closures to the south and is slightly more open to the north. It dips weakly to both the north and to the south. It extends 21 km with N-S to SSW-NNE orientation and is

confined between the La Hocha and Betania faults. To the north, it is cut by an unnamed reverse fault that follows a NE-SW direction, and to the south, it is cut by the Betania fault. The Saldaña Formation is located at its core, and the entire Cretaceous succession outcrops on its west flank, including the Olini Group and the Yaguará Formation, which have important phosphate layers (Figure 2e).

**El Vegón syncline.** This structure is smooth and has a vertical fold that dips weakly to both the SSW and to the north. The axis, both to the south and to the NNE, is cut by the Pacarní fault. Rocks from the Yaguará Formation comprise the outcrop in the core, and on the flanks, rocks from the Loma Gorda Formation and the Olini Group have a significant amount of phosphate levels.

**La Plata (Chusma) fault.** This is a high-angle reverse regional fault with SE tectonic transport. The hanging wall contains rocks from the Saldaña Formation and Jurassic plutons (e.g., Ibagué Batholith); this tectonic block rises over the Cretaceous and Paleogene sedimentary units (Figure 2f). The fault has 113 km length and is NE ( $29^\circ \pm 12^\circ$ ) oriented, with an average inclination of  $40^\circ$ - $60^\circ$  to the west and presents reverse-dextral-strike movement. This fault truncates important folds, such as the Nátaga anticline to the south and the Media Luna syncline to the north. It is recognized as the geological boundary between the Central Cordillera and the Neiva subbasin in the UMV (Butler and Schammel, 1988).

**San Francisco fault.** It is a low- to moderate-angle regional reverse fault ( $<45^\circ$  W), with a general NE orientation ( $10^\circ$ - $50^\circ$ ). The initial section brings into contact the Paleogene rocks of the Seca Formation and the Olini Group (in the hanging wall) with rocks from the Potrerillo Formation (in the footwall). To the north of the study area, the fault consists of fossilized Neogene rocks from the Honda Group. In the San Francisco fault, Cretaceous rocks of the Hondita Formation (in the hanging wall) are in contact with the rocks of the Yaguará Formation (in the footwall).

**Betania fault.** This regional reverse fault has a high dip angle ( $>45^\circ$  NW), and its main line follows a NE direction of  $40^\circ \pm 10^\circ$ . It extends for approximately 53 km, truncates the La Hocha anticline, and brings into contact rocks from the Saldaña Formation with Cretaceous and Paleogene-Neogene sedimentary rocks (Figure 2d).

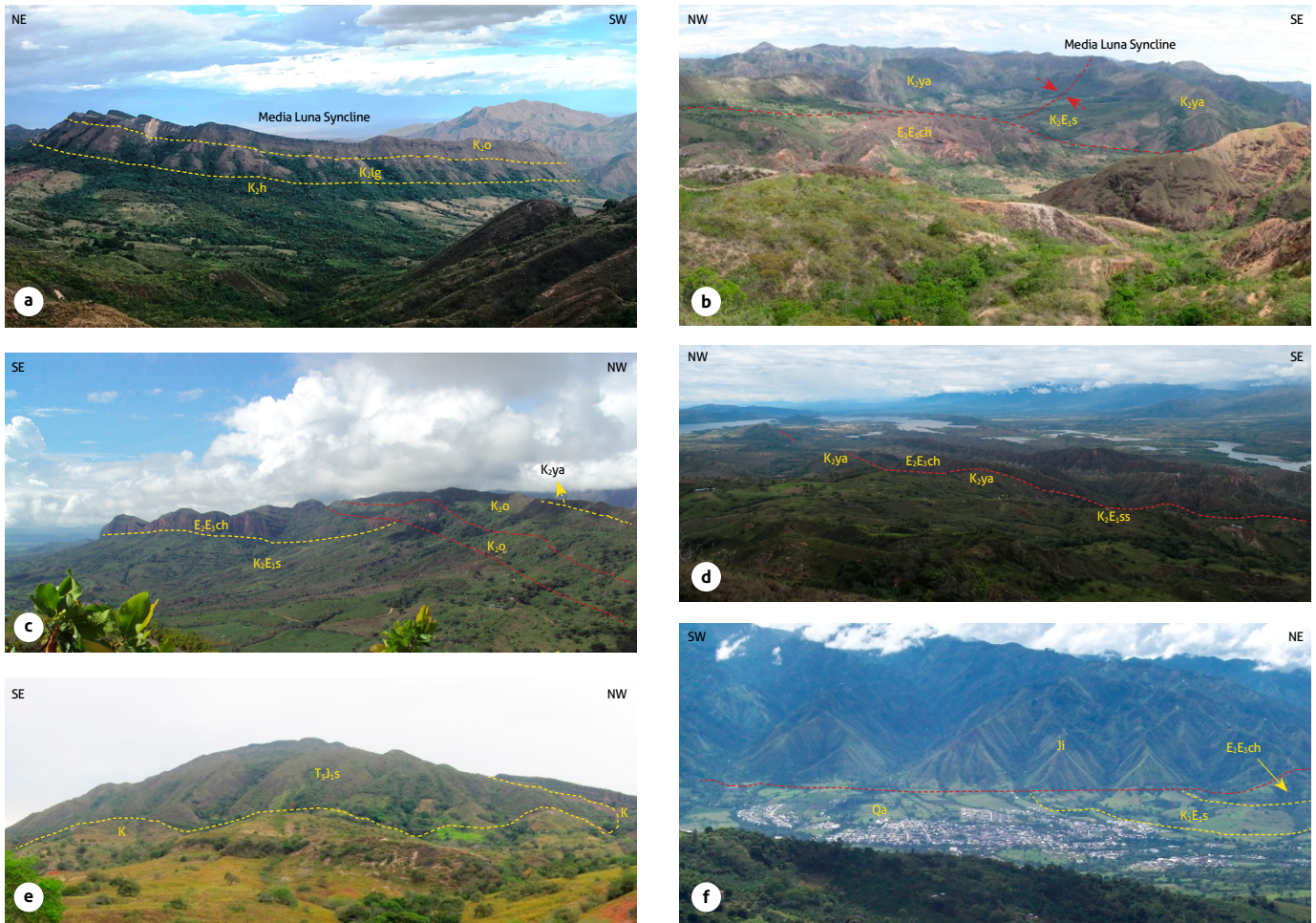


**Figure 2.** Main structures of the study area

a) Structural of the Media Luna syncline; rocks from the Hondita (K2h), Loma Gorda (K2lg) and Olini Group (K2o) formations are observed. b) La Plata (Chusma) fault, which truncates the continuity of the Media Luna syncline to the SSW and connects the Yaguará (K2ya) and Seca (K2E1s) formations to the Chicoral Formation (E2E3ch). c) San Francisco fault; which is where the Seca-Member Teruel formations (K2E1st) and Chicoral Formation (E2E3ch) connect with the Olini Group (K2o). d) Betania fault, which correspond to the contact between the Yaguará (K2ya) and Seca-Member San Francisco (K2E1ss) formations against the Chicoral Formation (E2E3ch). e) La Hocha anticline; rocks from the Saldaña Formation (T3J1s) crop out at the center of the structure and is covered by the basal Cretaceous succession (K). f) La Plata (Chusma) fault; is the tectonic contact between rocks from the Jurassic Ibagué Batholith (Ji) with rocks from the Seca (K2E1s) and Chicoral (E2E3ch) formations and is in the vicinity of the municipality of La Plata. Source: Terraza et al. (2019).

#### 4.2. Phosphate-bearing Upper Cretaceous lithostratigraphic units

The potential phosphate deposits are associated with the Lidita Inferior, Lidita Superior and Yaguará formations (*sensu* Terraza et al., 2019). Mapping these units is difficult due to the overlapping of tectonic events that caused strong deformation and impacted their geographic distribution and lateral continuity.

**Olini Group (K2o): Early Santonian-Campanian.** This group is widely distributed across the study area. Morphologically it stands out from the underlying Loma Gorda Formation, in the

sites where the overlying unit is the Yaguará Formation this stands out over the Olini Group (Figure 3). These features facilitated the geological mapping of this feature. The Olini Group was mapped along the Yaguaracito River (which lies on the eastern flank of the Nátaga anticline), from the north of Yaguará to Palermo (on both flanks of the La Hocha anticline), at the NE termination of the La Guagua anticline and to the SW of its eastern flank, in the center of the Nazareth syncline, on the western flank of the Media Luna syncline, and on its eastern flank, along the Aipe-Río Patá road. There is an outcrop associated with this group to the north and east of Paicol, in

the vicinity of the Paéz River. Additional outcrops are visible in narrow strips that follow a NE and NW direction located to the west and NW of Neiva, and in NNE-SSW direction from near Neiva and extending to the Aipe River, in the vicinity of the municipality of Aipe.

From bottom to top, the Olini Group consists of the Lidita Inferior Formation, the Aipe or Aico formations (*sensu* Terraza et al., 2019) and the Lidita Superior Formation.

In general, the Olini Group overlies the Loma Gorda formation and underlies the Yaguará formations with a sharp and conformable contact. The upper and lower contacts of the constituent formations (Lidita Inferior, Aipe or Aico and Lidita Superior) are also conformable and sharp.

**Yaguará Formation (K2ya): late Campanian-early Maastrichtian.** Outcrops of this formation are present on the eastern flank of the Nátaga anticline (Yaguaracito riverbed) and extends to the south toward the municipality of El Pital. This formation is also apparent in the center of the Itaibe syncline, which is located on the flanks of the La Hocha anticline and at the NE termination of the La Guagua anticline (which runs from the north of Yaguará to Palermo) where it continues to the SW of its eastern flank. It also crops out to the north and east of Paicol (in the vicinity of the Paéz River), to the west of Yaguará, to the west and NW of Neiva, and from the NW of Neiva to the Aipe River.

The Yaguará Formation was described in the stratigraphic section from the Yaguará River, where it presents an excellent exposure. Lithologically, it is composed of quartz-arenites that vary in texture from fine to very fine, and in color between brown, gray and yellow, with intercalations of mudstones,



**Figure 3.** Typical escarpments of the Yaguará Formation (K2ya) that overlie the Lidita Superior (K2ls) and Aico (K2ai) formations that comprise the Olini Group and underlie the Seca Formation  
Source: Terraza et al. (2019).

phosphates, porcelanites or quartz siltstones with glauconite, phosphate remains and dissolved calcareous concretions.

The Yaguará Formation underlies the Seca Formation, overlies the Lidita Superior Formation in sharp and concordant contact, and generates a prominent escarpment between these two units (see Figure 3). The Yaguará-Seca contact is considered a paraconformity (*sensu* Howe, 1997).

**Buscavida (K2b) and La Tabla (K2lt) formations: late Campanian-early Maastrichtian.** These formations emerge to the east of the La Plata (Chusma) fault in the area of the Media Luna syncline, which includes the Bambucá creek, where they have been previously described (SGC-UNAL Agreement, 2018). The morphological expression of the Buscavida Formation is of a narrow valley between the Lidita Superior and the La Tabla Formation, while the La Tabla Formation forms strong escarpments that are accentuated by the smooth landforms and topographic depressions generated by the mudstones and claystones of the overlying Seca formation.

To the south of the Bambucá creek, the exposed facies of the Buscavida (*sensu* Guerrero et al., 2000) and La Tabla formations change to the predominantly quartz-sandstone terrigenous lithofacies of the Yaguará Formation.

The Buscavida Formation overlies the Lidita Superior Formation and is in conformable sharp contact. Similarly, The Seca Formation overlies in concordant and sharp (paraconformable) contact the La Tabla Formation.

### 4.3. Phosphate-bearing Upper Cretaceous lithofacies

Table 1 shows the different facies in the Upper Cretaceous lithostratigraphic units that contain phosphates and correspond to the Santonian-Maastrichtian stratigraphic interval.

## 5. DISCUSSION

### 5.1. Facies characterization of the Santonian-Maastrichtian interval that contains phosphates

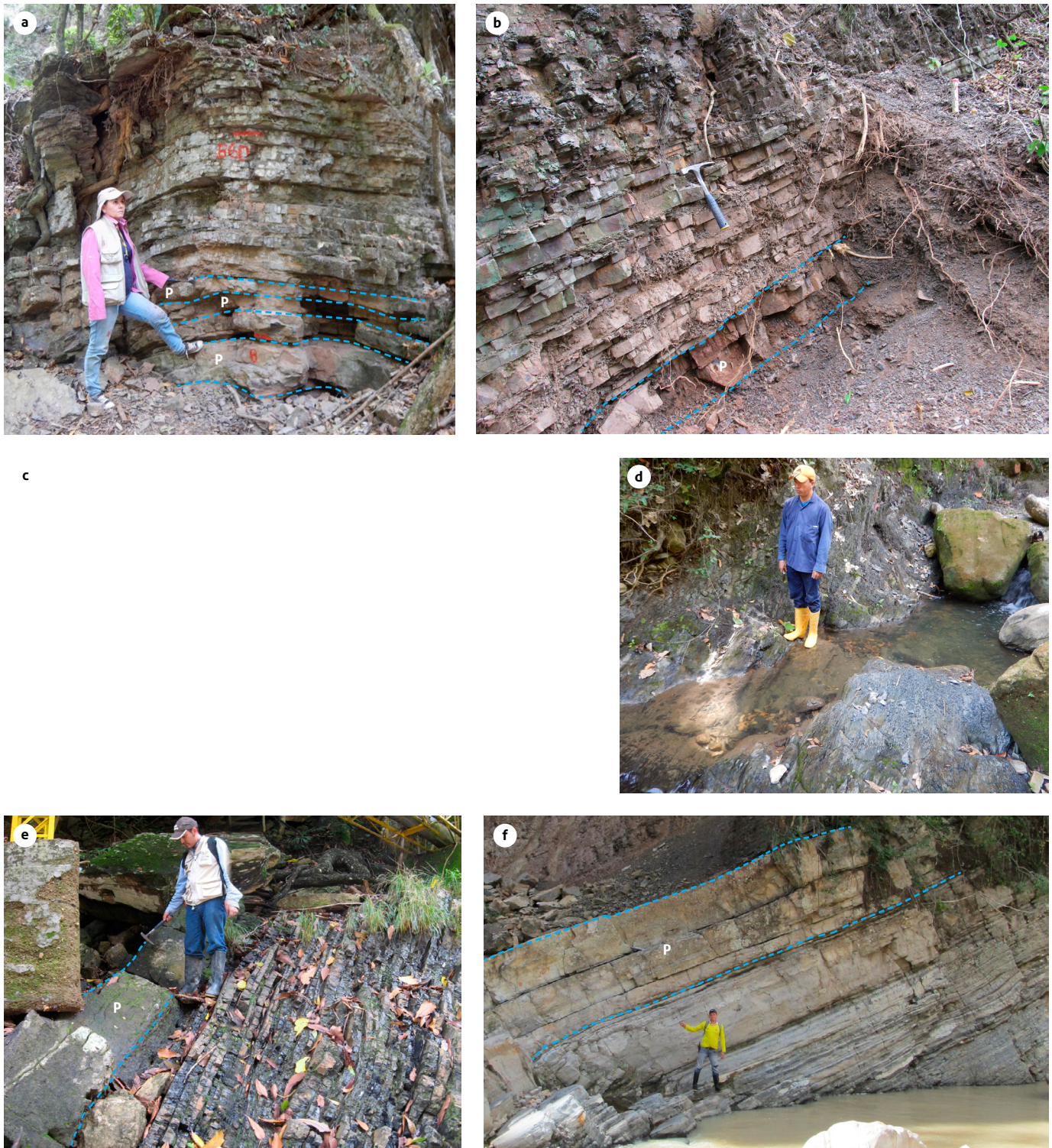
**Lidita Inferior Formation.** There is a predominance of chert facies to the north (Bambucá creek), where chert comprises 48% of the unit (Figure 4a). Toward the south, 35% of the unit consists of porcelanites with mudstone texture and phosphorites with peloids with packstone texture, while 12% of the unit consists of fish remains and phosphate clasts (Figure 4b). The phosphorite deposits are located toward the top of the unit. These phosphorite intervals can reach up to 90 cm in thick-

Table 1. Facies in the lithostratigraphic units that contain phosphates from the Upper Cretaceous (Santonian-Maastrichtian)

Unit	Facies and lamination	Stratification	Remarks	Associated Ichnofacies
Yaguará Formation	Very fine - fine grained sand, homogeneous appearance	Thick and very thick, Even nonparallel	Phosphates	<i>Teredolites, Thalassinoides</i>
	Very fine - fine grained sandstone, discontinuous wavy nonparallel	Thick and very thick. Even nonparallel	Calcareous	<i>Skolithos</i>
	Fossiliferous sands of medium grain, homogeneous appearance	Thick and very thick Curved, nonparallel	Calcareous with strong dissolution	<i>Thalassinoids</i>
	Very coarse-grained sandstone slightly conglomerate, cross-laminated, tangential to the base	Thick and very thick Curved, nonparallel		
	Quartz siltstones, Even parallel lamination	Medium and coarse, even parallel	Silicified	<i>Planolites</i>
	Porcelanite with Wackestone - mudstone texture, even parallel lamination	Thin and medium, even parallel	Fossiliferous-benthic foraminifera	
	Cherts with mudstone - wackestone texture, even parallel lamination	Thin, even parallel	Diagenetic Fossiliferous-Foraminifera Benthic Chert	
	Phosphorites with packstone and wackestone texture, homogeneous appearance	Thick and very thick, even nonparallel	Pellets, peloids, fish remains, phosphate intraclasts, benthic and planktonic foraminifera	
	Biosparites with grainstone-packstone texture, homogeneous appearance	Thick and very thick, curved parallel	Thick-shelled bivalves (ostreids), orientation of bioclasts	
	Biomicrorites with packstone texture, discontinuous, even nonparallel lamination	Medium and coarse, even nonparallel	Benthic foraminifera, bioclasts, peloids	
La Tabla Formation	Sandy biosparites with wackestone texture, Discontinuous, even nonparallel lamination	Coarse to very coarse, discontinuous, curved nonparallel	Remains of thick-shelled bivalves (ostreidae)	
	Fine-grained sands, cross-laminated, tangential to the base	Very thick, even parallel	Clayey	
	Medium-grained sands, cross-laminated, tangential to the base	Coarse to very coarse, Curved, nonparallel		
Buscavida Formation	Coarse to very coarse-grained sands, cross-laminated, tangential to the base	Coarse to very coarse, Curved, nonparallel		
	Terrigenous Mudstones, Even parallel lamination	Thin and medium, Even parallel		
Lidita Superior Formation	Fossiliferous sandy lodolites, Wavy, nonparallel lamination	Thin to medium Even parallel	Calcareous	<i>Planolites</i>
	Siltstones, Wavy, nonparallel lamination	Thin to medium, Even parallel		<i>Thalassinoids</i>
	Cherts with mudstone- wackestone texture, Even parallel lamination	Thin, Even parallel	Diagenetic chert, benthic foraminifera	
	Phosphorites with packstone and wackestone texture, homogeneous appearance	Coarse to very coarse, Wavy, parallel to discontinuous, curved, nonparallel	Pellets, peloids, fish remains, phosphate intraclasts, benthic and planktonic foraminifera	
	Porcelanite with wackestone - mudstone texture, Even parallel lamination	Thin and medium, Even parallel		
Aico Formation	Quartz siltstones, continuous Even parallel lamination	Thin, even parallel	Silicified, calcareous	
	Wackestone biomicrites, Wavy, parallel lamination	Thick, Wavy, parallel	Benthic and planktonic foraminifera, fish remains and peloids	
	Claystone with Discontinuous, wavy, nonparallel lamination	Thin and medium Discontinuous, even parallel	Pyritized Radiolaria	
	Terrigenous Mudstones with wavy nonparallel and discontinuous lamination	Thin even parallel		
Aipe Formation	Porcelanite with wackestone texture, Discontinuous, even parallel lamination	Medium, even parallel	Phosphates	
	Fine-grained sandstones with Wavy, nonparallel lamination	Medium, even parallel	Calcareous	<i>Palaeophycus</i>
Lidita Inferior Formation	Very fine and fine-grained sands, Wavy, nonparallel lamination	Thick and very thick, Even nonparallel	Locally lithic	
	Quartz siltstones, Even parallel lamination	Thin Even parallel	Silicified-calcareous	
	Porcelanite with mudstone texture, continuous parallel flat laminations	Continuous parallel plane, medium		
	Chert with mudstone -wackestone texture, even parallel lamination	Thin even parallel	Diagenetic chert, planktonic foraminifera	
Lidita Inferior Formation	Phosphorites with wackestone and packstone texture, homogeneous appearance	Medium and coarse, even parallel	Pellets, peloids, fish remains, phosphate intraclasts, benthic and planktonic foraminifera	
	Terrigenous Mudstones, even parallel lamination	Thin and medium even parallel	Silicified	

ness. In the southern part, they can be up to 30 cm thick (e.g., sections of El Caney, Río Íquira and Río Yaguaracito). The Lidita Inferior Formation in the Itaibe creek was correlated with

the upper middle part of the layer N-14 described by Mendiavelso (1982, 1993, Figure 3) and has a thickness of approximately 3 m.



**Figure 4.** Characteristics of the Olini Group in some stratigraphic sections  
a) Lidita Inferior Formation in the Yaya River stratigraphic section; porcelanites and cherts with phosphorite intercalations (P). b) Lidita Inferior Formation in the Íquira River stratigraphic section; thin layers of tabular porcelanite with a thin tabular layer of phosphorite (P) at the base. c) Aipe Formation in the Aipe River stratigraphic section comprised of very thick layers of quartz-arenites. d) Aico formation in the El Caney creek stratigraphic section, with fissile mudstones arranged in thin layers. e) Lidita Superior Formation in the Aipe River stratigraphic section; thin and medium subtabular layers of porcelanite with a thick wedged-shaped layer of phosphorite (P) interbedded. f) Lidita Superior Formation in the Íquira River stratigraphic section; medium layers of cherts with layers of phosphorite (P) on top. Source: Terraza et al. (2019).

**Aipe Formation.** The dominant facies of this formation (94% of the unit) consist of very thick layers of sandstone comprised of terrigenous sand (Figure 4c). However, the unit does not contain representative phosphate deposits. The thickness of the Aipe Formation in the Yaguaracito River is 26.3 m, and in the Aipe River, it is 76.6 m, displaying a thickening trend toward the north.

**Aico formation.** Typical clay facies represent 87% of this unit. However, fissile mudstones appear to a lesser extent, and occasionally hard levels of phosphatic porcelanite, very fine-grained sandstones and massive sandy limestone with packstone texture (Figure 4d). The Aico Formation is 20 m thick in the Caney creek, and 46.3 m thick in the Íquira River. Outcrops are mainly located in the southern part of the study area and in the east of the San Francisco fault. This unit was described in the stratigraphic sections from El Caney, Río Íquira, and partially in the Yaguará River. This unit represents a facial change for the Aipe Formation where these units are considered contemporary and heterotopic. The outcrops of the Aico Formation are 50 m thick in the Itaibe creek and correlate with the top of layer N14 described by Mendivelso (1982, 1993, Figure 3). The unit shows a tendency to thickening toward the SE (Figure 7).

**Lidita Superior Formation.** Chert facies with wackestone texture represent 38% of the unit, followed by peloidal phosphorites, which represent 29%, with packstone texture and wackestone, fish remains, planktonic and benthic foraminifera, layered with subtabular and canaliform shapes (Figures 4e and 4f). These facies do not exhibit internal laminations except at the base of the layers, where continuous nonparallel wavy laminations are seen. These have elongated and imbricated micritic intraclasts and decimetric chert nodules, spherical and ellipsoidal in size. Porcelanites, quartz-siltstones and some limestones compose 22% of the unit. The porcelanites are slightly calcareous, have wackestone and mudstone textures, and contain benthic and planktonic foraminifera arranged in very thin sheets. Additionally, phosphatic porcelanite with wackestone texture with benthic and planktonic foraminifera-bearing, peloids and fish remains are also found.

These beds are recurrent and are especially associated with phosphate levels. The laminations are interrupted by spherical chert nodules a centimeter in diameter and decimeter-scale ellipsoidal micritic concretions. Toward the top, it is common to observe phosphorite layers up to 70 cm thick with wackestone and packstone textures and wavy bases, which represent the most important accumulations of phosphates at the regional setting.

This unit shows a NE to SW thinning trend and has 31.6 m in thickness in the Bambucá creek and 9.4 m in the El Caney creek. In general, all the Upper Cretaceous units show this tendency; however, there is no correlation with the phosphate facies, as they are thicker toward the SW, possibly due to the proximity of the source area of the phosphate material.

**Yaguará Formation.** A total of 68.9% of the terrigenous facies are composed of quartz arenites; phosphatic quartz-arenites with peloids, phosphate clasts, glauconite and hydrocarbon inclusions; and fossiliferous friable quartz-arenites with centimeter-scale gastropod and bivalve remains and peloids (Figures 5a and 5b). Up to 24% of the terrigenous facies consist of phosphatic porcelanite and porcelanites with a mudstone and packstone texture, chert with a wackestone texture (with benthic and planktonic foraminifera) and siliceous siltstone (containing planktonic foraminifera and disseminated pyrite). Additionally, these units contain phosphatic siltstones that grade to very fine-textured phosphatic quartz-arenites, with siliceous cement, peloids and muscovite (Figure 5c). Regarding the relevant phosphate deposits, in the Divino Niño section to the NE of Paicol, there is a layer more than 2 m thick, which contains sandy phosphorite with a packstone texture (Figure 5d).

On the road between Hobo and Paicol, near the La Juanita phosphate mine, the La Juanita Member crops out, which is composed of calcareous facies likely deposited in a high energy environment. These facies consist of bivalve grainstone and fossilized sandy packstone, with sparitic cement, bivalve massif grainstone with articulated ostreid shells and sandy wackestone with weathered pale yellowish orange sparitic cement. Furthermore, all the beds in these facies are either conformable or oriented obliquely to the stratigraphy. These facies represent approximately 20% of the unit in this section (Figures 5e and 5f).



**Figure 5.** Main characteristics of the Yaguará Formation in some stratigraphic sections  
 a) Aipe River stratigraphic section; thick and very thick layers of quartz-arenites in which cavities are observed due to the dissolution of calcareous concretions. b) The Yaguará River stratigraphic section; thick and very thick layers of phosphatic quartz-arenites in which cavities were formed due to dissolution of calcareous concretions and interspersed with thin layers of porcelanite and siltstones. c) Íquira River stratigraphic section; very fine-textured quartz-arenites overlaid by siliceous siltstones. d) Divino Niño stratigraphic section; phosphorites (P) with packstone texture. e) La Juanita stratigraphic section; bivalve grainstones in thick and solid layers in the middle part of the La Juanita Member. f) La Juanita stratigraphic section; grainstone to packstone containing ostreidae shown in detail at the bottom of the La Juanita Member. Source: Terraza et al. (2019).

Thickness of the Yaguará Formation is variable. This formation is thicker to the east of the study area. It is 134 m thick in the El Boquerón creek (Palermo municipality), 99 m in the typical section of the Yaguará River and 78 m in the Íquira River. The narrowest parts of the formation were registered in the Yaguaracito River, where it was on 19 m wide. In the Itai-be creek, the Yaguará Formation is approximately 150 m thick

and is correlated with the N-12 to N-5 layers of the Campanian and N-4 to N-1 of the Maastrichtian, as designated by Mendivelso (1982, 1993, Figure 3) for the Guadalupe Group.

The Yaguará Formation represents the facies change of the Buscavida and La Tabla formations, and for this reason it is assigned an equivalent age to these two units, which varies between the late Campanian and the early Maastrichtian.

## 5.2. Facies analysis of the Santonian-Maastrichtian interval that contains phosphates

Based on the interpretation of the facies and the lithocorrelations that have been carried out, the possible hydrodynamic conditions that prevailed on the sea floor during the accumulation of the phosphate-rich sediments in the Santonian-Maastrichtian period are inferred. For this interpretation, a generic morphological profile of a modern ramp-type coastal depositional system was taken as a reference, compiled from the published specialized literature (Figure 6).

The sediments observed in the facies from the Lidita Inferior and Lidita Superior formations accumulated on very low sloping sea floors, which is reflected in the parallel flat stratification of these units, and under low-energy and dysoxic conditions. This conclusion is suggested by the predominance of thinly laminated fine-granular facies arranged in a parallel and flat sequence and the absence of any bioturbation. Thus, these sediments belonged to a medium carbonate ramp environment, and were below the fair-weather wave action but above the baseline of storm-driven waves.

In the Lidita Inferior and Lidita Superior formations, sedimentation was influenced by waves and bottom currents,

which is expressed within the phosphate lithofacies. These lithofacies present slightly wavy stratification and lamination, parallel and nonparallel, canaliform layers, decreases in grain size, a low to moderate degree of bioturbation, and rounded and imbricated particles. The observed lithofacial characteristics support reworking processes by unidirectional marine currents induced by tides, normal waves and the energetic action of storm waves. In the case of the Lidita Inferior Formation, an enrichment in organic matter is observed (>1%), which suggests that accumulation occurred with minimal benthic oxygen levels (e.g., at the sediment-water interface, or a few centimeters below), which would have prevented oxidation and subsequent bacterial destruction. The appearance of benthic foraminifera is an indication of shallower conditions in the sedimentary environment, possibly toward the upper part of the middle ramp (upper offshore).

The Aipe and La Tabla formations, represented by clayey to silty sandstone, with grain sizes that vary from very fine to granule, correspond to moderate to high energy environments. Additionally, these environments contained active benthic organisms (with high degrees of bioturbation), had wavy to sloped laminations, and thick to very thick layers. These characteristics

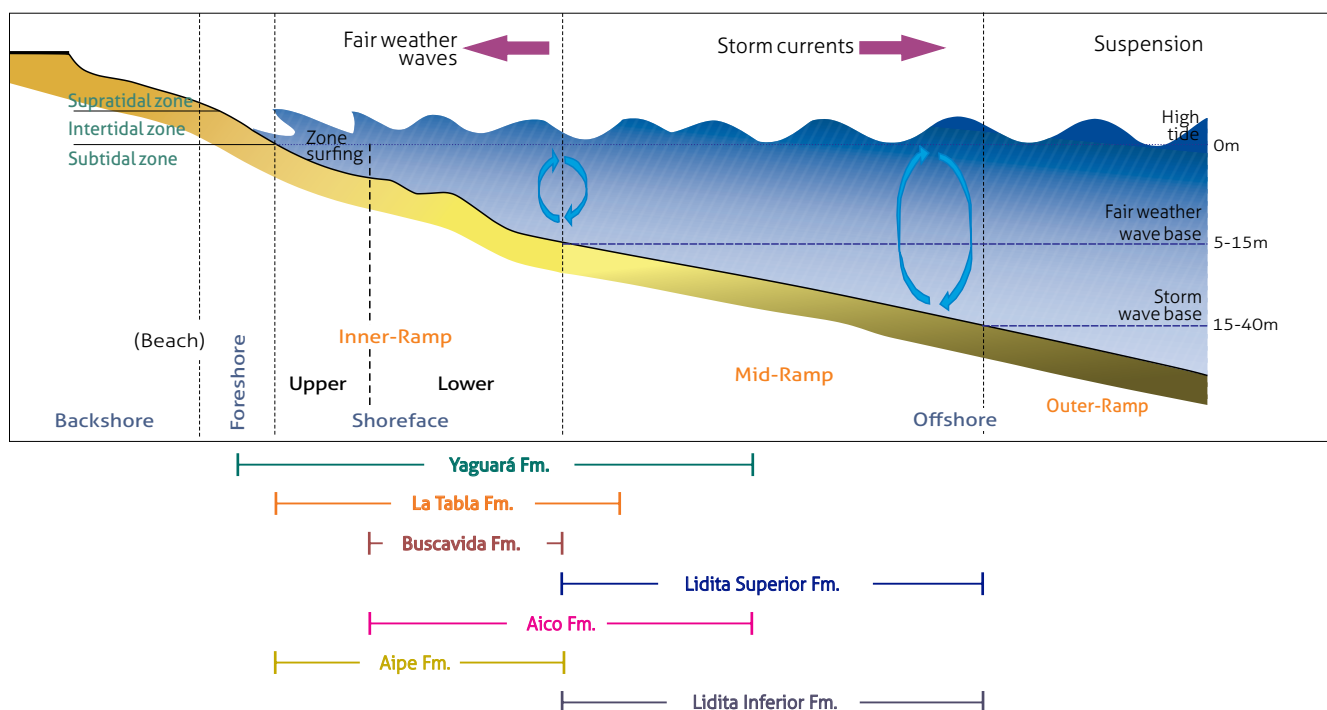


**Figure 6.** Interpreted sedimentary environment corresponding to the different Upper Cretaceous facies Based on Flügel and Munnecke (2010), Reineck and Singh (1980); Walker and Plint (1992); Evoy and Moslow (1995); Zelazny et al. (2018).

indicate an upper to lower shoreface depositional environment on an oxygenated bottom along the internal ramp.

The Buscavida Formation is characterized by facies that indicate environments with moderate to low energies, possibly indicative of hydrodynamic conditions along an internal ramp environment in the lower shoreface (Reineck and Singh, 1980). This interpretation is based on heterolytic laminations, the abundance of benthic foraminifera and the presence of burrows. Furthermore, it is common for sandstones and mudstones to be associated with calcareous deposits during periods of low terrigenous contribution. The hydrodynamic conditions inferred from the facies of the Aico Formation are similar, albeit shallower, to those of the Lidita Superior and Lidita Inferior formations, as evidenced by the benthic fauna and the sedimentary structures observed, probably associated with a lagoonal environment.

Finally, the Yaguará Formation presents facial variations that indicate variable hydrodynamic energy. With a predominance of sandstone facies with grain sizes that vary from very fine to fine, wavy laminations, layers with textural variations between coarse and very coarse, and evidence of high degrees of bioturbation (indicating locally complete disturbance) by the vigorous action of benthic organisms within the substrate. The energy of this environment ranged from moderate to high and likely represents a lower to upper shoreface configuration on an oxygenated bottom on the internal ramp. The fine-granular facies were thinly laminated, in parallel, and interspersed with siltstones, which suggests accumulation occurred in the middle ramp on a sea floor with low levels of hydrodynamic energy and below the action of the waves during good weather.

The La Juanita Member of the Yaguará Formation contains large accumulations of bioclastic carbonates (grainstone and packstone) and canaliform layers of disarticulated oysters, with its long axis parallel to the stratification, which suggests that accumulation occurred in high energy areas with intense biological activity that were subjected to waves and unidirectional currents. This area was possibly a well oxygenated intertidal and subtidal zone that was located between the upper shoreface and the foreshore (Reineck and Singh, 1980).

### 5.3. Basin paleotopography for the phosphate-bearing Santonian-Maastrichtian interval

Based on the lithocorrelation of the Upper Cretaceous stratigraphic sections (Figures 7 and 8), for which a baseline was taken at the contact between the Yaguará and Seca formations,

the possible paleotopography of the basin in the western sector of the Neiva subbasin of the UMV that corresponds to the Santonian and Maastrichtian periods, is inferred.

The distribution, shape and thickness of the observed facies, as well as the lithostratigraphic units involved, allow us to suggest that tectonism conditioned the landforms of the basin floor. This tectonic activity was probably related to the uplift pulses of the ancient Central Cordillera during the Campanian and Maastrichtian periods (Salazar, 1992; Villamil, 1998; Velozza et al., 2008; Roncancio and Martínez, 2010; Bayona, 2018; Villamizar et al., 2021).

The uplift triggered a subsidence deformation mechanics that led to the creation of foreland basins (Jordan, 1995; Flemings and Jordan, 1990, Horton et al., 2010) and facilitated deposition within a tectonic post-graben environment (Föllmi et al., 1992, Horton et al., 2010). This dynamic tectonic framework allowed certain faults to control the accommodation space and the sediment accumulation conditions along the bottoms as well as the paleotopographic configuration of the sedimentary environments of the units studied here. This resulted in zones with differential subsidence essentially controlled by regional tectonics. As a product of this tectonism, there are synchronous and heterotopic lithostratigraphic units that show marked variability in terms of thickness and facies, as is the case of the Aipe vs. Aico and the Yaguará vs. Buscavida and La Tabla formations.

Depending on the intensity and periodicity of the tectonic uplift, there were periods in which the sedimentation was relatively more stable, which added to the relative eustatic sea level conditions and allowed the Lidita Inferior and Lidita Superior formations to be deposited in less dynamic environments. These units present facies associated with a relative rise in sea level with low rates of sharp accumulation of sediments under low energy conditions, as evidenced by their sedimentary structures.

Concomitantly, physicochemical mechanisms were developed that favored the supply and mobilization of nutrients, which led to the increase in bioproductivity that was necessary for phosphogenesis. Subsequently, the pristine phosphate generated was remobilized and concentrated by waves and bottom currents in layers of “granular” phosphates (sensu Glenn et al., 1994) or “allochthonous” phosphates (sensu Föllmi et al., 1992; Föllmi, 1996) in the Lidita Superior and Lidita Inferior Formations. The most likely accumulation mechanism would have occurred through storm-induced gravity sediment

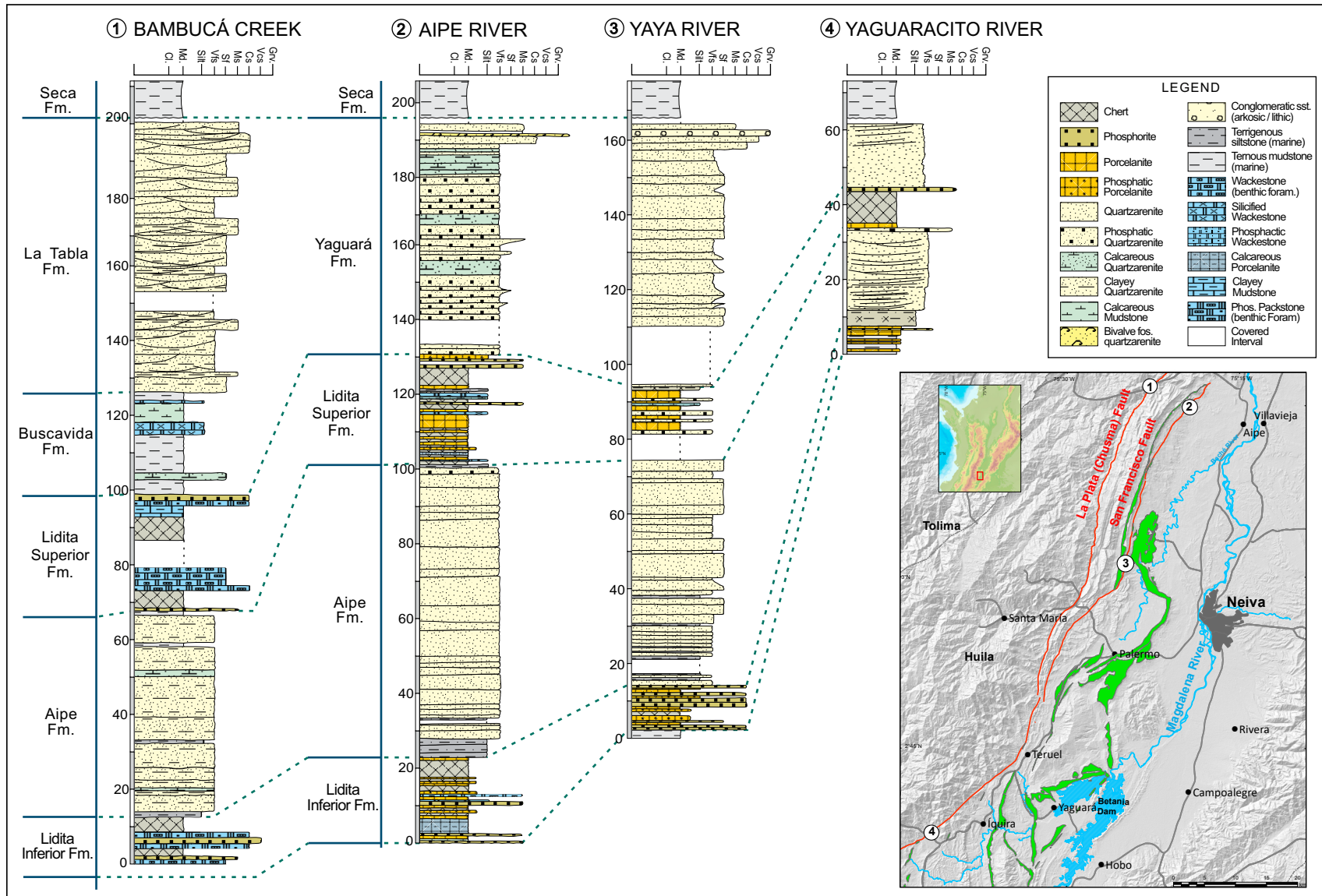


Figure 7. Lithocorrelation in the NE-SW direction within the western portion of the study area

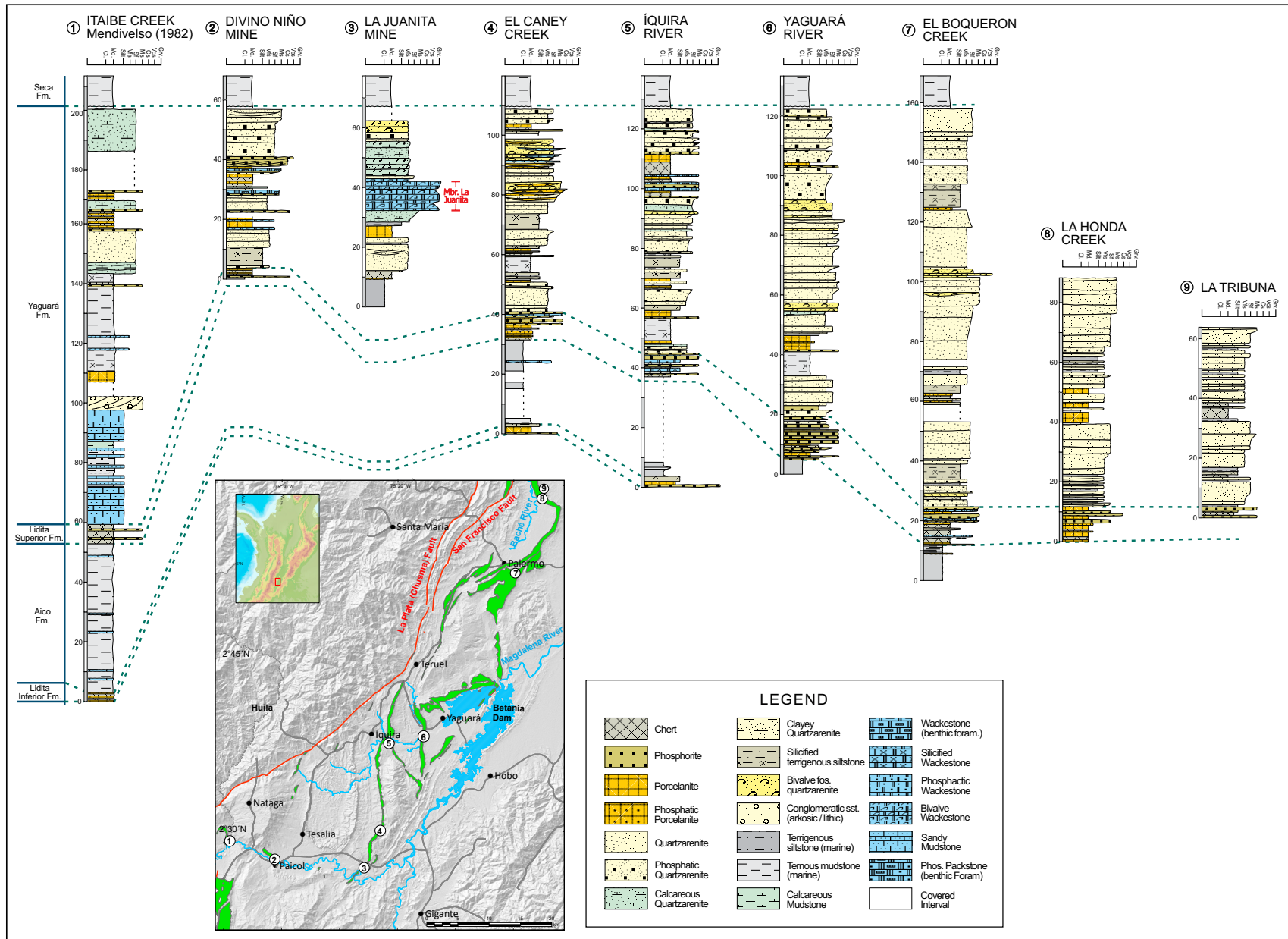


Figure 8. Lithocorrelation along the west to east orientation in the study area

flows. These flows were generated between the base level of the waves in both calm and stormy weather. Then, the flows amalgamated successively to form the layers of granular or allochthonous phosphate, which are the thickest and most economically interesting phosphate deposits in Colombia and worldwide (Grimm, 2000; Pufahl et al., 2003).

The accumulation mechanism of phosphorites associated with quartz-arenite rocks, such as those found in the Yaguará Formation (e.g., in the Divino Niño stratigraphic section, in NE Paicol, see Figure 4d), was possibly similar; the difference is in the hydrodynamic and depth conditions. To explain these coastal phosphorites, a rapid accumulation of granular phosphates is inferred in littoral areas due to storms, a process analogous to that described by Brenner and Davis (1973) to explain underdeveloped sand bars in intertidal plains. This type of deposit shows little lateral continuity, as confirmed by the geological mapping carried out in the surroundings of the El Divino Niño phosphate mine to the NE of Paicol. Furthermore, these deposits were specifically conditioned by the morphology of the bottom and the dynamics of the flow that mobilized them.

By comparing the thicknesses of the Upper Cretaceous lithostratigraphic units in the SN direction in the west of the study area (Figure 7), a thickening is observed oriented along the NE direction, which varies from slightly more than 60 m in the Yaguaracito River section to more than 200 m in the Bambucá creek section. This thickening trend is evident throughout the entire UMV basin, as reported by Vergara (1997) and Mora (2003), who affirm that the increase in accommodation space in the units to the north of the basin is notable, which allows for a greater accumulation of sediment.

It is feasible to consider that the sea floor on which these units were deposited did not present a continuous form but instead showed landforms, or a paleotopography, that would have controlled the thickness and distribution of the sediments, as well as the hydrodynamic conditions that impacted the sediments and the sedimentary environments. These interpretations can be inferred from the lithocorrelation that was carried out in the study area along the east to west orientation, (Figure 8).

It is inferred that toward the end of the Maastrichtian, there was a paraconformity (*sensu* Howe, 1997) between the deposits within the Yaguará or La Tabla formations and the Seca Formation. This is evidenced by the marked change from the fluvial environments in the Seca Formation to the reddish mudstones

and claystones of the marine facies from the upper shoreface as shown by the Yaguará or La Tabla Formations. Geological mapping shows that the Yaguará Formation, on the western flank of the La Hocha anticline, is gradually losing thickness along the north-south direction because the uppermost layers of the unit are progressively eroding, which confirms the proposed hypothesis. Roncancio and Martínez (2010) related this event to the first uplift pulses of the Central Cordillera, which initiated the folding of the sedimentary sequence in the UMV basin.

## 6. CONCLUSIONS

The detailed geological mapping and stratigraphic descriptions made it possible to specify that the Upper Cretaceous Lidita Inferior, Lidita Superior and Yaguará formations contain the phosphate layers of major economic interest, which correspond to phosphorites with packstone texture. The vertical and lateral distribution of these layers is conditioned by the compressive and transpressive structural style with dominant tectonic transport toward the east. This gave rise to the folding of the lithostratigraphic units of the Santonian-Maastrichtian interval where the phosphates are hosted. Furthermore, the deposits are truncated by regional faults, such as the La Plata (Chusma) and San Francisco faults, which complicate the modeling of these deposits.

The La Plata (Chusma) fault is considered the geological limit between the Central Cordillera and the Neiva subbasin in the UMV. The San Francisco fault is another important structure that truncates folds and the lithostratigraphic units where the phosphate deposits are found. Some of the main fold axes are curvilinear (e.g., the Tesalia syncline and La Hocha anticline) because the pre-Cretaceous basement affects the geomorphology of the structures.

The sedimentary components, textures and structures observed in the phosphorites suggest that sediment transport and accumulation was influenced by bottom currents and storm-induced waves through gravity flows or rapid accumulation of sediments in littoral sand bars in medium to very shallow marine environments. Likewise, the Upper Cretaceous facies (Santonian-Maastrichtian period) represented in the Lidita Inferior, Aipe, Aico, Lidita Superior, Yaguará, Buscavida and La Tabla formations suggest a shallow, ramp-like marine environment, with the seabed less than 40 m below the surface. Additionally, accumulation occurred from the transition zone to the upper shoreface to the middle ramp offshore. High ener-

gy storms, such as hurricanes and typhoons, syndepositionally reworked the pristine phosphate lithofacies, which later accumulated as allochthonous phosphorites (Föllmi et al., 1992; Föllmi, 1996) or granular phosphorites (Glenn et al., 1994).

The successive amalgamation of granular, or allochthonous, phosphate layers produced thicker deposits of greater economic interest (Grimm, 2000; Pufahl et al., 2003). These types of layers are the ones that appear in the study area and must have formed during the periods of maximum storm activity, thus generating phosphorites with packstone texture.

The distribution, shape and thickness of the facies observed in the Upper Cretaceous units that correspond to the Santonian-Maastrichtian interval, which appear as outcrops in the western regions of the Neiva subbasin, allow us to infer tectonism and exhumation of the source areas concomitant with sedimentation. This type of dynamic environment allowed certain faults to control the sediment accommodation space, the hydrodynamic conditions of the seafloor and the paleotopography of the basin, which resulted in zones with differential subsidence essentially controlled by regional tectonics.

#### ACKNOWLEDGMENTS

This research was carried out as part of the Phosphates and Magnesium Prospecting and Exploration project, code: 1001615, Dirección de Recursos Minerales of the SGC. The authors express their gratitude to Dr. Gloria Prieto Rincón for her full support and to Dr. Fernando Etayo Serna for his advice on the chronostratigraphy of the different lithostratigraphic units that were mapped. We thank the anonymous reviewers and the Editorial Committee of the *Boletín Geológico* of the SGC for their comments and suggestions. Finally, we thank the geographer Hernán Cifuentes for his determined technical support to the working group.

#### REFERENCES

- Bayona, G., García, D., & Mora, G. (1994). La Formación Saldaña: producto de la actividad de estratovolcanes continentales en un dominio retro-arco. In F. Etayo Serna (dir.), *Estudios geológicos del Valle Superior del Magdalena*. Universidad Nacional de Colombia. W. Taller Editorial Ltda.
- Bayona, G. (2018). El inicio de la emergencia en los Andes del norte: una perspectiva a partir del registro tectónico-sedimentológico del Coniaciano al Paleoceno. *Revista de la Academia Colombiana de Ciencias Exactas, Físicas y Naturales*, 42(165), 364-378. <http://dx.doi.org/10.18257/raccefyn.632>
- Beltrán, N., & Gallo, J. (1968). *The geology of Neiva Sub-Basin Upper Magdalena Basin, southern portion*. Ninth Annual Field Conference. Colombian Society of Petroleum Geologists and Geophysicists.
- Brenner, R. L., & Davis, K. D. (1973). Storm-generated coquina sandstone: Genesis of high-energy marine sediments from the Upper Jurassic of Wyoming and Montana. *GSA Bulletin*, 84(5), 1685-1698. [https://doi.org/10.1130/0016-7606\(1973\)84<1685:SCSGOH>2.0.CO;2](https://doi.org/10.1130/0016-7606(1973)84<1685:SCSGOH>2.0.CO;2)
- Bürgl, H., & Botero, D. (1967). Las capas fosfáticas de la cordillera Oriental. *Boletín Geológico*, 15(1-3), 7-44. <https://doi.org/10.32685/0120-1425/bolgeol15.1-3.1967.88>
- Bustamante, C., Archanjo, C. J., Cardona, A., & Vervoort, J. D. (2016). Late Jurassic to Early Cretaceous plutonism in the Colombian Andes: A record of long-term arc maturity. *GSA Bulletin*, 128(11-12), 1762-1779. <https://doi.org/10.1130/B31307.1>
- Butler, K., & Schamel, S. (1988). Structure along the eastern margin of the Central Cordillera, Upper Magdalena Valley, Colombia. *Journal of South American Earth Sciences*, 1(1), 109-120. [https://doi.org/10.1016/0895-9811\(88\)90019-3](https://doi.org/10.1016/0895-9811(88)90019-3)
- Cáceres, C., Cediell, F., & Etayo, F. (2003). *Mapas de distribución de facies sedimentarias y armazón tectónico de Colombia a través del Proterozoico y del Fanerozoico*. Ingeominas.
- Campbell, C. (1967). Lamina, laminaset, bed and bedset. *Sedimentology*, 8(1), 7-26. <https://doi.org/10.1111/j.1365-3091.1967.tb01301.x>
- Compton, R. (1985). *Geology in the field*. John Wiley & Sons, Inc.
- Conpes 3577 (2009). *Política nacional para la racionalización del componente de costos de producción asociado a los fertilizantes en el sector agropecuario*. Departamento Nacional de Planeación.
- Conpes 3577 (2009). *Política nacional para la racionalización del componente de costos de producción asociado a los fertilizantes en el sector agropecuario*. Departamento Nacional de Planeación.
- Cathcart, J., & Zambrano, F. (1967). Roca fosfática en Colombia, con una sección sobre fosfatos de Turmequé, Boyacá. *Boletín Geológico*, 15(1-3), 65-162. <https://doi.org/10.32685/0120-1425/bolgeol15.1-3.1967.210>
- Cook, P., & Shergold, J. (1986). Proterozoic and Cambrian phosphorites: An introduction. In *Phosphate deposits of the*

- World, vol. 1: Proterozoic and Cambrian phosphorites. Cambridge University Press.
- Dunham, R. (1962). Classification of carbonate rocks according to depositional texture. In W. E. Ham (ed.), *Classification of Carbonate Rocks, a Symposium* (pp. 108-121). American Association of Petroleum Geologists. <https://doi.org/10.1306/M1357>
- Etayo, F. (1994). A modo de historia geológica del Cretácico en el valle superior del Magdalena. In F. Etayo Serna (dir.), *Estudios geológicos del Valle Superior del Magdalena*. Universidad Nacional de Colombia.
- Evoy, R. W., & Moslow, T. F. (1995). Lithofacies associations and depositional environments in the Middle Triassic Doig Formation, Buick Creek Field, northeastern British Columbia. *Bulletin of Canadian Petroleum Geology*, 43(4), 461-475. <https://doi.org/10.35767/gscpgbull.43.4.461>
- Flemings, P. B., & Jordan, T. E. (1990). Stratigraphic modeling of foreland basins: Interpreting thrust deformation and lithospheric rheology. *Geology*, 18(5), 430-435. [https://doi.org/10.1130/0091-7613\(1990\)018<0430:SMOFBI>2.3.CO;2](https://doi.org/10.1130/0091-7613(1990)018<0430:SMOFBI>2.3.CO;2)
- Flórez, M., & Carrillo, G. (1994). Estratigrafía de la sucesión litológica basal del Cretácico del valle superior del Magdalena. In F. Etayo Serna (dir.), *Estudios geológicos del valle superior del Magdalena*. Universidad Nacional de Colombia.
- Flügel, E., & Munnecke, A. (2010). *Microfacies of carbonate rocks: Analysis, interpretation and application*. Springer.
- Folk, R. (1951). Stages of textural maturity in sedimentary rocks. *Journal of Sedimentary Research*, 21(3), 127-130. <https://doi.org/10.2110/jsr.21.127>
- Folk, R. (1954). The distinction between grain size and mineral composition in sedimentary-rock nomenclature. *The Journal of Geology*, 62(4), 344-359. <https://doi.org/10.1086/626171>
- Folk, R. (1959). Practical petrographic classification of limestones. *The American Association of Petroleum Geologists Bulletin*, 43(1), 1-38. <https://doi.org/10.1306/0BDA5C36-16BD-11D7-8645000102C1865D>
- Folk, R. (1962). Spectral subdivision of limestone types. In W. E. Ham (ed.), *Classification of Carbonate Rocks, a Symposium* (pp. 62-84). American Association of Petroleum Geologists. <https://doi.org/10.1306/M1357>
- Folk, R., & Siedlecka, A. (1974). The "schizohaline" environment: its sedimentary and diagenetic fabrics as exemplified by Late Paleozoic rocks of Bear Island, Svalbard. *Sedimentary Geology*, 11(1), 1-15. [https://doi.org/10.1016/0037-0738\(74\)90002-5](https://doi.org/10.1016/0037-0738(74)90002-5)
- Folk, R. (1980). *Petrology of sedimentary rocks*. Hemphill Publishing Co.
- Föllmi, K. B. (1990). Condensation and phosphogenesis: Example of the Helvetic mid-Cretaceous (northern Tethyan margin). Special Publications, vol. 52. Geological Society of London. <https://doi.org/10.1144/GSL.SP.1990.052.01.17>
- Föllmi, K. B. (1996). The phosphorus cycle, phosphogenesis and marine phosphate-rich deposits. *Earth-Science Review*, 40(1-2), 55-124. [https://doi.org/10.1016/0012-8252\(95\)00049-6](https://doi.org/10.1016/0012-8252(95)00049-6)
- Föllmi, K. B., Garrison, R. E., Ramírez, P. C., Zambrano Ortiz, F., Kennedy, W. J., & Lehner, B. L. (1992). Cyclic phosphate-rich successions in the Upper Cretaceous of Colombia. *Palaeogeography, Palaeoclimatology, Palaeoecology*, 93(3-4), 151-182. [https://doi.org/10.1016/0031-0182\(92\)90095-M](https://doi.org/10.1016/0031-0182(92)90095-M)
- Fürsich, F. (1995). Shell concentrations. *Eclogae Geologicae Helveticae*, 88(3), 643-655.
- Glenn, C., Föllmi, K., Riggs, S., Baturin, G., Grimm, K., Trappe, J., Abed, A., Galli-Olivier, C., Garrison, R., Ilyin, A., Jehl, C., Rohrlich, V., Rushdi, Sadaqah, R., Schidlowski, M., Sheldon, R., & Siegmund, H. (1994). Phosphorus and phosphorites: Sedimentology and environments of formation. *Eclogae Geologicae Helveticae*, 87(3), 747-788.
- Grimm, K. A. (1997). Phosphorites feed people. *Farm Folk/City Folk's Newsletter*, (13), 4-5.
- Grimm, K. A. (2000). Stratigraphic condensation and the redeposition of economic phosphorite: Allostratigraphy of Oligo-Miocene shelfal sediments, Baja California Sur, Mexico. In C. R. Glenn, L. Prévôt-Lucas & J. Lucas (eds.), *Marine Authigenesis: From Global to Microbial*. Society for Sedimentary Geology. <https://doi.org/10.2110/pec.00.66.0325>
- Guerrero, J., Sarmiento, G., & Navarrete, R. (2000). The stratigraphy of the W. side of the Cretaceous Colombian Basin in the Upper Magdalena Valley: Reevaluation of selected areas and type localities including Aipe, Guaduas, Ortega, and Piedras. *Geología Colombiana*, 25, 45-110.
- Hampson, G., & Storms, J. E. (2003). Geomorphological and sequence stratigraphic variability in wave-dominated, shoreface-shelf parasequences. *Sedimentology*, 50(4), 667-701. <https://doi.org/10.1046/j.1365-3091.2003.00570.x>
- Hernández, J., & Uruña, C. (2017). Aspectos geocronológicos y petrogenéticos del Complejo Aleluya: implicaciones en la exploración de Mg en el norte del departamento del Huila, Colombia. *Memorias XVI Congreso Colombiano de Geología*, Santa Marta, August 28 to September 1, 2017.

- Horton, B. K., Saylor, J. E., Nie, J., Mora, A., Parra, M., Reyes-Harker, A., & Stockli, D. F. (2010). Linking sedimentation in the northern Andes to basement configuration, Mesozoic extension, and Cenozoic shortening: Evidence from detrital zircon U-Pb ages, Eastern Cordillera, Colombia. *GSA Bulletin*, 122(9-10), 1423-1442. <https://doi.org/10.1130/B30118.1>
- Howe, R. (1997). Geologic contacts. *Journal of Geoscience Education*, 45(2), 133-136. <https://doi.org/10.5408/1089-9995-45.2.133>
- Ingram, R. (1954). Terminology for the thickness of stratification and parting units in sedimentary rocks. *GSA Bulletin*, 65(9), 937-938. [https://doi.org/10.1130/0016-7606\(1954\)65\[937:TFTTOS\]2.0.CO;2](https://doi.org/10.1130/0016-7606(1954)65[937:TFTTOS]2.0.CO;2)
- Jiménez, G., Rico, J., Bayona, G., Montes, C., Rosero, A., & Sierra, D. (2012). Analysis of curved folds and fault/fold terminations in the southern Upper Magdalena Valley of Colombia. *Journal of South American Earth Sciences*, 39, 184-201. <https://doi.org/10.1016/j.jsames.2012.04.006>
- Jordan, T. E. (1995). Retroarc Foreland and related basins. In C. J. Busby & R. V. Ingersoll (eds.), *Tectonics of sedimentary basins* (pp. 331-362). Blackwell Science.
- Julivert, M. (1970). Cover and basement tectonics in the Cordillera Oriental of Colombia, South America, and a comparison with some other folded chains. *GSA Bulletin*, 81(12), 3623-3646. [https://doi.org/10.1130/0016-7606\(1970\)81\[3623:CAB-TIT\]2.0.CO;2](https://doi.org/10.1130/0016-7606(1970)81[3623:CAB-TIT]2.0.CO;2)
- Kamola, D., & Van Wagoner, J. (1995). Stratigraphy and facies architecture of parasequences with examples from the Spring Canyon Member, Blackhawk Formation, Utah. In *Sequence Stratigraphy of Foreland Basin Deposits: Outcrop and Subsurface Examples from the Cretaceous of North America*, AAPG Memories vol. 64. American Association of Petroleum Geologists. <https://doi.org/10.1306/M64594C3>
- Kammer, A., Piraquive, A., Gómez, C., Mora, A., & Velásquez, A. (2020). Structural styles of the Eastern Cordillera of Colombia. In *The geology of Colombia*, vol. 3. Servicio Geológico Colombiano. <https://doi.org/10.32685/pub.esp.37.2019.06>
- Krumbein, W., & Sloss, L. (1969). *Estratigrafía y sedimentación*. Uteha.
- Mendivelso, D. (1982). *Aspectos fotogeológicos y estratigráficos del Cretáceo en la región de Itaiibe (valle superior del Magdalena)* (Bachelor thesis). Universidad Nacional de Colombia.
- Mendivelso, D. (1993). Aspectos fotogeológicos y estratigráficos del Cretáceo por la quebrada Itaiibe, valle superior del río Magdalena, Colombia. *Revista Cipres*, 14(1), 67-84.
- Miall, A. D. (1984). Variations in fluvial style in the lower Cenozoic synorogenic sediments of the Canadian Arctic Islands. *Sedimentary Geology*, 38(1-4), 499-523. [https://doi.org/10.1016/0037-0738\(84\)90091-5](https://doi.org/10.1016/0037-0738(84)90091-5)
- Mojica, P. (1987). Fosfatos. In *Recursos minerales de Colombia* (t. II, pp. 856-893). Ingeominas.
- Mojica, J., & Franco, R. (1990). Estructura y evolución tectónica del valle medio y superior del Magdalena, Colombia. *Geología Colombiana*, 17, 41-64.
- Moore, D., & Scruton, P. (1957). Minor internal structures of some recent unconsolidated sediments. *American Association of Petroleum Geologists Bulletin*, 41(12), 2723-2751. <https://doi.org/10.1306/0bda59db-16bd-11d7-8645000102c1865d>
- Mora, A. (2003). *Modelo estratigráfico para el Cretácico Basal (Aptiano-Albiano) en el norte de la subcuenca de Neiva, valle superior del Magdalena, Colombia*. 8.º Simposio Bolivariano, Exploración Petrolera en las Cuencas Subandinas. European Association of Geoscientists and Engineers.
- Morales, C., Caicedo, J., Velandia, F., & Núñez, T. (2001). *Geología de la plancha 345, Campoalegre: Memoria explicativa*. Ingeominas.
- Nichols, G. (1999). *Sedimentology and Stratigraphy*. Blackwell Science.
- Notholt, A. J. G. (1985). Phosphorite resources in the Mediterranean (Tethyan) phosphogenic province: A progress report. *Sciences Géologiques, Bulletins et Mémoires*, 77(1), 9-17.
- Powers, M. (1953). A new roundness scale for sedimentary particles. *Journal of Sedimentary Research*, 23(2), 117-119. <https://doi.org/10.1306/0bda59db-16bd-11d7-8645000102c1865d>
- Ptáček, P. (2016). Phosphate rocks. En *Apatites and their synthetic analogues: Synthesis, structure, properties and applications*. IntechOpen. <https://doi.org/10.5772/59882>
- Pufahl, P. K., Grimm, K. A., Abed, A. M., & Sadaqah, R. M. (2003). Upper Cretaceous (Campanian) phosphorites in Jordan: Implications for the formation of a south Tethyan phosphorite giant. *Sedimentary Geology*, 161(3-4), 175-205. [https://doi.org/10.1016/S0037-0738\(03\)00070-8](https://doi.org/10.1016/S0037-0738(03)00070-8)
- Reineck, H., & Singh, I. (1980). *Depositional sedimentary environments (with reference to terrigenous clastics)* (2.ª ed.). Springer-Verlag.
- Reineck, H., & Wunderlich, F. (1968). Classification and origin of flaser and lenticular bedding. *Sedimentology*, 11(1-2), 99-104. <https://doi.org/10.1111/j.1365-3091.1968.tb00843.x>
- Rodríguez, G., Arango, M. I., Zapata, G., & Bermúdez, J. G. (2018). Petrotectonic characteristics, geochemistry, and U-Pb geochronology of Jurassic plutons in the Upper Magdalena

- Valley-Colombia: Implications on the evolution of magmatic arcs in the NW Andes. *Journal of South American Earth Sciences*, 81, 10-30. <https://doi.org/10.1016/j.jsames.2017.10.012>
- Roncancio, J., & Martínez, M. (2010). Upper Magdalena Basin. In F. Cediél & F. Colmenares (eds.), *Petroleum geology of Colombia*, vol. 14. Agencia Nacional de Hidrocarburos.
- Salazar, A. (1992). *Depositional and paleotectonic settings of the Cretaceous sequence, Upper Magdalena Valley, Colombia*. S. A. (Ph. D. thesis). University of South Carolina.
- Sarmiento Rojas L. F. (2019). Cretaceous stratigraphy and paleo-facies maps of Northwestern South America. In F. Cediél & R. P. Shaw (eds.), *Geology and tectonics of Northwestern South America*. Frontiers in Earth Sciences. Springer. [https://doi.org/10.1007/978-3-319-76132-9\\_10](https://doi.org/10.1007/978-3-319-76132-9_10)
- Servicio Geológico Colombiano, & Universidad Nacional de Colombia. (2018). Convenio Especial de Cooperación n.º 13 de 2017. Potencial de fosfatos en un sector del valle superior del Magdalena mediante el estudio estratigráfico de las rocas cretácicas, haciendo énfasis en el Cretáceo superior.
- Soudry, D., Glenn, C. R., Nathan, Y., Segal, I., & VonderHaar, D. (2006). Evolution of Tethyan phosphogenesis along the Northern edges of the Arabian-African shield during the Cretaceous-Eocene as deduced from temporal variations of Ca and Nd isotopes and rates of P accumulation. *Earth-Science Reviews*, 78(1-2), 27-57. <https://doi.org/10.1016/j.earscirev.2006.03.005>
- Swanson, R. (1981). *Sample examination manual*. AAPG Methods in Exploration Series, vol. 1. The American Association of Petroleum Geologists. <https://doi.org/10.1306/Mth1413>
- Terraza, R. (2019). "Formación La Luna": expresión espuria en la geología colombiana. In F. Etayo-Serna (dir.), *Estudios geológicos y paleontológicos sobre el Cretácico en la región del embalse del río Sogamoso, Valle Medio del Magdalena*. Compilación de los Estudios Geológicos Oficiales en Colombia, vol. XXIII. Servicio Geológico Colombiano. <https://doi.org/10.32685/9789585231788-5>
- Terraza, R., Martin, C., Martínez, G., & Rojas, N. (2016). *Exploración geológica de fosfatos en el Bloque Boyacá, planchas 191 y 210*. Informe técnico. Servicio Geológico Colombiano.
- Terraza, R., Martin, C., Martínez, G., Rojas, S., & Rojas, N. (2019). *Exploración geológica de fosfatos en el departamento del Huila, costado occidental del río Magdalena. Planchas 302, 323, 344, 345 y 366*. Informe técnico. Servicio Geológico Colombiano.
- Terraza Melo, R., Martin Rincón, C. L., Martínez Aparicio, G. A., Rojas Jiménez, S. T., Rojas Parra, N. R., & Hernández González, J. S. (2019). *Litoestratigrafía estandarizada para el valle superior del Magdalena, subcuena de Neiva, costado W del río Magdalena*. Publicaciones Especiales del Servicio Geológico Colombiano.
- The Geological Society of America. (1995). *Rock-color chart*. Prepared by The Rock-Color Chart Committee, 8<sup>th</sup> printing.
- United States Geological Survey-USGS. (2022). *Mineral commodity summaries 2022*. U.S. Geological Survey, 202 p. <https://doi.org/10.3133/mcs2022>
- Van Wagoner, J., Mitchum, R., Campion, K., & Rahmanian, V. (1990). Siliciclastic sequence stratigraphy in well logs, cores and outcrops: Concepts for high-resolution correlation of time and fades. *AAPG Methods in Exploration Series*, (7), 55.
- Veloza, G, Mora, A., De Freitas, M., & Mantilla, M. (2008). Dislocación de facies en el tope de la secuencia cretácica de la subcuena de Neiva, valle superior del Magdalena, y sus implicaciones en el modelo estratigráfico secuencial colombiano. *Boletín de Geología*, 30(1), 29-44.
- Vergara, L. (1997). Stratigraphy, foraminiferal assemblages and paleoenvironments in the late Cretaceous of the Upper Magdalena Valley, Colombia (part I). *Journal of South American Earth Sciences*, 10(2), 111-132. [https://doi.org/10.1016/S0895-9811\(97\)00010-2](https://doi.org/10.1016/S0895-9811(97)00010-2)
- Villamil, T. (1998). Chronology, relative sea-level history and a new sequence stratigraphic model for basinal Cretaceous facies of Colombia. In L. James & C. D. Pindell (eds.), *Paleogeographic Evolution and Non-Glacial Eustasy, Northern South America* (pp. 161-216). Special publication vol. 58. SEPM Society for Sedimentary Geology.
- Villamizar, N., Bernet, M., Urueña, C., Hernández, J. S., Terraza, R., Roncancio, J., & Piraquive, A. (2021). Thermal history of the Southern Central Cordillera and its exhumation record in the Cenozoic deposits of the Upper Magdalena Valley, Colombia. *Journal of South American Earth Sciences*, 107, 103-105. <https://doi.org/10.1016/j.jsames.2020.103105>
- Walker, R. G., & Plint, A. G. (1992). Wave and storm dominated shallow marine systems. In R. G. Walker & N. P. James (eds.), *Facies models: Response to sea-level change* (pp. 219-238). Geological Association of Canada.
- Wilkins, A. D. (2011). *Terminology and the classification of fine-grained sedimentary rocks: Is there a difference between a claystone, a mudstone and a shale?* University of Aberdeen.

- Williams, H., Turner, F., & Gilbert, C. (1954). *Petrography: An introduction to the study of rocks in thin sections*. W. H. Freeman & Company, Inc.
- Zapata, S., Cardona, A., Jaramillo, J. S., Patiño, A., Valencia, V., León, S., Mejía, D., Pardo-Trujillo, A., & Castañeda, J. (2019). Cretaceous extensional and compressional tectonics in the Northwestern Andes, prior to the collision with the Caribbean oceanic plateau. *Gondwana Research*, 66, 207-226. <https://doi.org/10.1016/j.gr.2018.10.008>
- Zambrano, F., & Mojica, P. (1990). Characteristics of Colombian phosphate deposits. In G. E. Ericksen, M. T. Cañas Pinochet & J. A. Reinemund (eds.), *Geology of the Andes and its relation to hydrocarbon and mineral resources*. Circum-Pacific Council for Energy and Mineral Resources Earth Science Series, v. 11.
- Zelazny, I. V., Gegolick, A., Zonneveld, J. P., Playter, T., & Moslow, T. F. (2018). Sedimentology, stratigraphy and geochemistry of Sulphur Mountain (Montney equivalent) Formation outcrop in south central Rocky Mountains, Alberta, Canada. *Bulletin of Canadian Petroleum Geology*, 66(1), 288-317.